AD-A087 343 DEFENCE RESEARCH ESTABLISHMENT ATLANTIC DARTMOUTH (NO--ETC F/G 20/4
MODEL SCALE EFFECTS ON A 16-309 FLAPPED HYDROFOIL SECTION.(U)
APR 80 E A JONES
UNCLASSIFIED DREA-TM-80/B NL

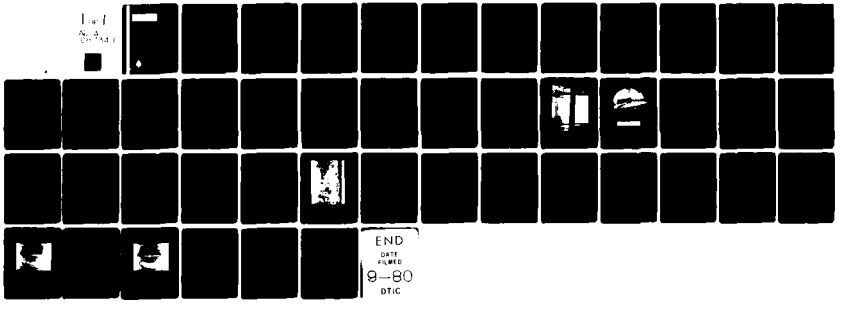

END
DATE FILMED
9-80
DTIC

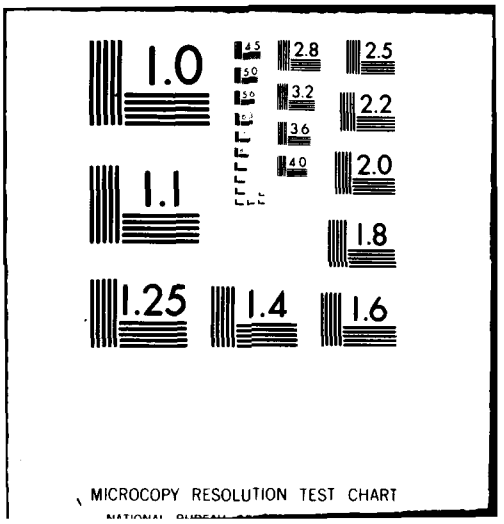
1.0
1.1
1.25
1.4
1.6
1.8
2.0
2.2
2.5
2.8
3.2
3.6
4.0
4.5
5.0
5.6
MICROCOPY RESOLUTION TEST CHART

DEFENCE RESEARCH ESTABLISHMENT
ATLANTIC

MODEL SCALE EFFECTS ON A 16-309 FLAPPED HYDROFOIL SECTION

D.R.E.A. TECHNICAL MEMORANDUM 80/8

RESEARCH AND DEVELOPMENT BRANCH
DEPARTMENT OF NATIONAL DEFENCE
CANADA

RESEARCH AND DEVELOPMENT BRANCH
DEPARTMENT OF NATIONAL DEFENCE
CANADA

DEFENCE RESEARCH ESTABLISHMENT
ATLANTIC
DARTMOUTH N.S.

(14) DREA-TM

(2) D.R.E.A. TECHNICAL MEMO[redacted] 80/B

(6)

MODEL SCALE EFFECTS ON A 16-309 FLAPPED HYDROFOIL SECTION.

(10) Eric [redacted] A. Jones

(11) April [redacted] 80

(12) 46

Approved by J. R. BROWN A/Director / Technology Division

DISTRIBUTION APPROVED BY

CHIEF D. R. E. A.

RESEARCH AND DEVELOPMENT BRANCH
DEPARTMENT OF NATIONAL DEFENCE
CANADA

ABSTRACT

Wind and water tunnel tests have been conducted of a NACA 16-309 section with the standard a = 1.0 camber line and equipped with a 25% flap-chord ratio, simple, sealed flap. Differences between test results from the two facilities are discussed, as well as the effect of placing roughness strips near the leading edge. Results are given showing the dependency of force, moment and, in partiular, cavitation inception on Reynolds number over the range from 1.25×10^6 to 4.0×10^5.

To to the 6th power

SOMMAIRE

On a fait subir à une section du profil aérodynamique NACA 16-309 (code de référence normalisé a 1.0) munie d'un volet hypersustentateur étanche simple ayant un rapport volet/corde de profil de 25% des essais en galerie hydraulique et en galerie aérodynamique. On discute des différences qui existent entre les résultats obtenus dans l'une et l'autre des installations ainsi que des effets produits par la mise en place de bandes de résistance près du bord d'attaque. On présente les résultats ayant trait à la force de sustentation, au moment et, en particulier, à la cavitation sur une gamme de nombres Reynolds allant de 1.25×10^6 à 4.0×10^6.

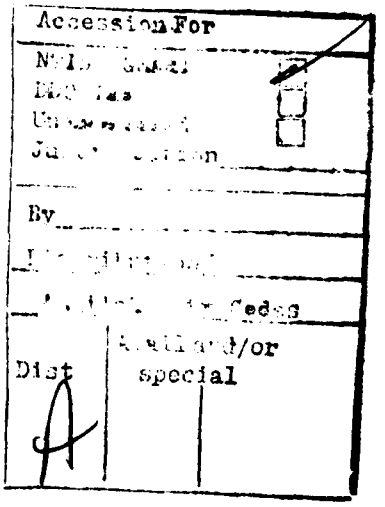

TABLE OF CONTENTS

NOTATION

C_d	section drag coefficient
C_ℓ	section lift coefficient
C_m	section quarter chord pitching moment coefficient
$C_p min$	minimum pressure coefficient
Re	Reynolds number
α	angle of attack
δ	flap angle
σ	cavitation number

1. INTRODUCTION

The NACA 16 Series family of airfoil sections has found considerable use in fully-submerged hydrofoil systems, both with incidence control and with a simple, sealed, trailing edge flap for control purposes. Favourable cavitation characteristics make these sections attractive for high-speed, subcavitating hydrofoil design, but this usefulness is offset to some extent by a susceptibility to trailing edge flow separation. These sections are designed to have a low drag at moderate subsonic Reynolds numbers by maintaining an extensive laminar flow. However, at Reynolds numbers appropriate to full-scale hydrofoil applications (approaching 5×10^7), the flow will be turbulent over most of the section.

In order to investigate flapped hydrofoils of this type, two-dimensional wind and water tunnel tests were made on a 16-309 section with the standard a = 1.0 camber-line and a 25% flap-chord ratio. The wind tunnel tests[1] were made on a 30 inch chord model in the 6 ft by 9 ft wind tunnel of the National Aeronautical Establishment, Ottawa. Two series of water tunnel tests[2] took place in the High Speed Circulating Water Tunnel of the Graduate Aeronautical Laboratories at the California Institute of Technology, Pasadena.

The wind tunnel tests and the first of the water tunnel test series have been reported separately[1,2]. They show a large measure of agreement but there are significant differences. There are also inconsistencies between the cavitation inception data measured in the two water tunnel test series. It is with these differences and inconsistencies that this report is largely concerned.

The maximum full chord Reynolds number that could be obtained in either test facility was about 4×10^6, a value at least an order of magnitude lower than is typical for a full size hydrofoil. The comparatively small model test values were of concern because boundary layer flow conditions and cavitation inception are both sensitive to Reynolds number, making scaling errors likely. Wind tunnel data were taken at two Reynolds numbers in order to allow some assessment of this. In the water tunnel, the sensitivity of force, moment and cavitation inception data to Reynolds number variation was investigated. However, because of limited available tunnel time, these tests were performed for only a very few combinations of data. Subsequently, the cavitation dependence data were augmented by a second series of water tunnel tests which included tests with roughness strips to stimulate turbulence transition at the leading edge.

2. MODELS AND TEST PROGRAM

2.1 Models and Measurements

Both the wind and water tunnel tests were two-dimensional, with the models occupying the full span of each test facility. The wind tunnel model, shown in Figure 1, was 6 feet in span, 30 inches in chord and made of solid aluminum. The size of the model enabled it to be constructed with great accuracy and to incorporate a fine grid of pressure ports for detailed measurement of the pressure distribution over the main body and over the trailing edge flap. Lift and pitching moment measurements were made using the wind tunnel dynamometer. Drag measurements reported here were obtained from a wake survey at center span since this is an inherently accurate method, unaffected by interference and other errors which can affect drag measurements by dynamometer.

The much smaller, six-inch span, stainless steel model shown in Figure 2 was tested in the C.I.T. High Speed Water Tunnel, using the two-dimensional test section[3]. This test section is 50 inches long by 30 inches high by 6 inches span and was specially developed for investigating the section characteristics of hydrofoils, particularly cavitation. For these tests, lift, drag and pitching moment were also measured, but the small size of the model and the general difficulties of water tunnel dynamometer measurements gave lower accuracies than the wind tunnel.

Drag was considered the most difficult measurement in the water tunnel because it is a low value measurement made in the presence of comparatively high lift and pitching moment values. Moreover, it is necessary to correct for significant tare forces originating at the model base. This base was a six inch diameter disc which mounted the model to the dynamometer and which was arranged to fit flush with and form part of the tunnel wall. A further complication resulted from the unavoidable gap between the free end of the model and the opposite tunnel wall. This gap measured 0.030 inch at atmospheric pressure for most data presented here but was reduced to 0.020 inch for some experiments. The width of the gap changed as tunnel pressure was increased or decreased to control the cavitation number of the flow.

The profile accuracies of the wind and water tunnel models, given for center span but typical of the measurements as a whole, are compared in Figure 3 on the basis of the profile error-to-chord ratio. It is difficult to obtain high profile accuracy at reasonable cost in the comparatively small stain-

less steel models used in the water tunnel. In absolute terms, the profile accuracies of the two models are not greatly different, but expressed as a percentage of maximum chord, the wind tunnel model is clearly superior. The surface finish of both models was judged to be fair and smooth, but, again due to its small size, the water tunnel model was probably proportionally the rougher.

2.2 Reynolds Numbers and Test Conditions

Wind tunnel measurements were made mainly at the two Reynolds numbers of 1.90×10^6 and 4.05×10^6 and covered the ranges of -10° to +15° flap angle and -4° to 6° angle of attack (Table 1). Most of the initial series of water tunnel tests (Series I) were made at a nominal Reynolds number of 2.5×10^6, but in addition, for four angle settings given by 0° and 2° angle of attack (α) and 0° and 5° flap angle (δ), tests in this series were made at Reynolds numbers of 1.25, 2.0, 2.5, 3.5 and 4.0 x 10^6 (Table 2). The object of these latter tests was to determine the Reynolds number sensitivities both of cavitation occurrence and of the measured forces and moments. The Series II water tunnel tests, made to augment these sensitivity data, were concerned with cavitation occurrence only. Observations were made for 1° increments of angle of attack over the range from -4° to +4° and at the two flap angles of 0° and 5°. Reynolds numbers ranged between 1.25×10^6 and 4.20×10^6 (Table 3).

In the interval between the Series I and Series II tests, the water tunnel was equipped with a new honeycomb flow-straightening element. As a result, flow turbulence was reported by CIT to have decreased from 0.08% to an extremely low value of 0.03%, as measured in the general purpose test section. Air content also decreased somewhat from about 13 parts per million in Series I, to about 10 parts per million in Series II. The wind tunnel turbulence value has been given[4] as between 0.1 and 0.2%.

3. FORCE AND MOMENT DATA

3.1 Wind Tunnel Measurements

As noted in the introduction, the flow is turbulent over most of the section at full-scale Reynolds numbers. At the test Reynolds numbers, however, the point of transition is only just starting to move forward of the pressure recovery region near the trailing edge with, in consequence, an enhanced sensitivity of the boundary layer to small changes in Reynolds number or flow conditions. This makes scaling and extrapolation to full scale Reynolds numbers impossible. The conventional

solution to these problems, adopted in these tests, is to locate transition tripping devices, such as roughness strips, near the leading edge of the section.

The section lift characteristics are seen from Figure 4 to exhibit marked discontinuities in the transition-free condition, that is, without the addition of roughness strips. It is apparent that sharp loss of lift occurred once a certain critical angle of attack was exceeded, particularly at the higher test flap angles. There was also a small but systematic change in these critical angles of attack when Reynolds number was changed from 4.0 to 1.9×10^6.

Sharp increase of C_d with C_ℓ on laminar flow sections is classically associated with a sudden forward shift in the location of the transition point. There is no significant loss of lift so long as the flow remains attached but in this case, transition shift is accompanied by flow separation at the trailing edge of the flap. The flow separation, indicated by oil flow visualisation studies and by surface pressure distribution plots, develops on either the upper or lower surface of the trailing edge, depending on the angle of attack and flap settings.

The transition-free drag characteristics are shown in the drag polar diagram, Figure 5. Data points on the curves corresponding to angle of attack have been omitted for clarity, but it can be seen that the values of lift on each curve at which the drag sharply increases correspond to the inflections in the lift characteristics shown in Figure 4.

Roughness strips were added at 5% chord on the upper and lower surfaces, for flap angles of 0° and 6°, to fix the transition point close to the leading edge (the "transition-fixed" condition) and establish the flow as turbulent. The resulting lift values are shown in Figure 4 to form a smooth projection of the upper part of the lift characteristics, that is, the part for which turbulent flow conditions are known already to apply.

Oil flow visualisation studies were made at 6° flap angle with transition-fixed, to determine the flow separation characteristics for turbulent flow conditions. These showed flow separation to occur on the upper surface of the trailing edge down to the lowest test angle of attack of -4°. They also showed the point of separation to advance smoothly along the chord as angle of attack increased.

Transition will occur more readily under the higher Reynolds number and more turbulent conditions normally encountered by a hydrofoil in a seaway. Thus, under practical ocean conditions, it is reasonable to expect a comparatively smooth onset of trailing edge separation and avoidance of the sharp discontinuities characteristic of the transition-free wind tunnel tests.

3.2 Comparison of Wind and Water Tunnel Data

Lift, drag and quarter chord pitching moment data are compared in Figures 6, 7 and 8 respectively. The small degree of cavitation which occurs at the data values indicated by arrows probably increases the lift values slightly but is not important to this discussion. The wind tunnel measurements at 6° and -4° flap angle have been interpolated where necessary for direct comparison with water tunnel measurements made at ±5° flap angle. No artificial turbulence stimulation was used for any of these water tunnel force and moment measurements.

The lift characteristics of Figure 6 show that the water tunnel data are generally in agreement with the wind tunnel data, provided boundary layer flow conditions are taken into account. For the 5° flap angle case, the water tunnel lift data are intermediate between the transition-fixed and transition-free wind tunnel values over the lower part of the angle of attack range. This suggests that flow separation occurred more readily in the water tunnel, and data for the 0° and 10° flap angle cases are also consistent with this. In turn, increased flow separation on the water tunnel model suggests a degree of turbulent flow not achieved on the wind tunnel model under similar, transition-free conditions. One possible reason is that the degree of turbulence in the water tunnel flow was actually higher than thought, due to deterioration of the honeycomb flow straightening element. A second possible cause is the proportionally poorer accuracy and surface finish of the water tunnel model.

Figure 7 shows large differences between the wind and water tunnel drag data, the water tunnel measurements being much higher over most of the C_ℓ range, regardless of the wind tunnel boundary layer flow condition. As noted briefly in Section 2.1 and described more fully in Reference 2, there were difficulties in measuring the comparatively low drag forces by dynamometer in the water tunnel. The drag measurements made by wake survey in the wind tunnel are considered inherently more reliable, and the water tunnel drag data have been largely discounted.

Quarter chord pitching moment, shown in Figure 8 as a function of lift coefficient for flap angles of 0°, 5° and

10°, is dependent primarily on the effective camber. It will therefore be influenced both by flap angle and by the degree of flow separation. The data show a good measure of agreement where flow conditions were assumed to be similar. The comparatively sharp changes in pitching moment exhibited by the transition-free wind tunnel model are consistent with the lift changes attributed in Section 3.1 to flow separation over the trailing edge of the flap.

3.3 Reynolds Number Dependence of Force and Moment Data

Lift and quarter chord pitching moment are shown as functions of Reynolds number in Figures 9 and 10 for the wind and water tunnel models. Again there is a large measure of agreement between the data from the two facilities when boundary layer flow conditions are taken into account. This is demonstrated for example in the $0°\alpha$, $5°\delta$ case, where the water tunnel boundary layer evidently changes from laminar to turbulent over the Reynolds number test range, with resulting flow separation. In the $2°\alpha$, $5°\delta$ case, the level of the values and their comparative lack of variation indicate that flow is separated and that the point of separation is stationary over the whole of the Reynolds number test range. In the two 0° flap angle cases, there is little change of lift and Figure 6 shows that any lift changes resulting from flow separation at $0°\delta$ will be small. Nevertheless, more distinct evidence of changes due to transition and flow separation might have been expected in the water tunnel data, particularly in the $0°\alpha$, $0°\delta$ case.

4. CAVITATION DATA

4.1 Test Conditions

Data on the effect of Reynolds number on cavitation inception are more extensive than for lift and pitching moment, due to the Series II tests which were made expressly to investigate this more thoroughly. As noted in Section 2.2, the tunnel was equipped with a new honeycomb flow-straightening element in the interval between the Series I and Series II tests. As a result, the free stream flow turbulence in the two-dimensional test section almost certainly underwent a substantial decrease. Whether from this or other causes, Series II leading edge cavitation inception numbers with natural transition were often significantly lower than Series I.

Roughness strips were applied at the leading edge to stimulate transition in an attempt to improve data consistency. Application proved difficult because the strips deteriorated

rapidly in the high speed flows. As a result, most data were restricted to the 0° flap angle case and to Reynolds numbers of 3.05×10^6 or less, although some data were collected for the 5° flap angle case and for Reynolds numbers up to 3.98×10^6.

The strips had to be applied 4 times, giving the cases marked A, B, C and D in the data plots. The dimensions of the strip were intentionally varied for case D. The inner 2 inches of model span (the balance end) was invariably left smooth; the center 2 inches invariably had .002 inch spherical glass beads top and bottom over the first 1.3% of the chord; the outer 2 inches (the free end) had .005 inch spherical glass beads top and bottom over the first 2% of the chord for application D.

A typical bead dispersion pattern is shown in Figure 11. A dispersion of about 10% by area was sought, but coverage was somewhat variable and generally a little higher than this. The center 2 inches of span tended to cavitate marginally more readily than the outer, even though the bead size was smaller. The data exhibited some scatter and some apparent differences for different roughness strip applications but these are considered more likely due to observation difficulties and uncontrolled experimental differences than to systematic changes in the roughness characteristics.

The test method was to lower the tunnel pressure slowly until full cavitation occurred or until cavity oscillations became excessive, and then to increase the pressure slowly. Visual observations were made of the pressures at which cavitation inception and desinence occurred at the leading edge, upper surface mid-back (approximately 50% chord) and upper surface hinge-line. In some cases, cavitation occurred at two locations simultaneously. Only the cavitation inception indices are plotted, partly to avoid complication of the plots and partly because of difficulty in judging the effective point of desinence.

4.2 Discussion of Results

The results for 0° flap angle are shown in Figures 12 to 21 for angles of attack of 4°, 3°, 2°, 1°, 0°, -1°, -2° and -4°; and for the 5° flap angle case, for 2° and 1° angle of attack. Minimum pressure coefficient values ($-C_{p_{min}}$) from the wind tunnel tests, which theoretically correspond with the cavitation inception numbers, have been included for comparison.

Leading edge upper surface cavitation cases are shown in Figures 12, 13, 14, 20 and 21. The $2°\alpha$, $0°\delta$ case of Figure 14 is the only leading edge case for which systematic data are

available for Series I and Series II water tunnel tests, transition-fixed and -free. For Series I data, there is increasing agreement with the wind tunnel $-C_p$min values as Reynolds number increases and considerable inconsistency at the main test Reynolds number of 2.5×10^6. The transition-free Series II data for the same case were consistently much lower than the Series I data; at low Reynolds number, the location of the cavitation even changed from the leading edge to mid-back and hinge-line. The addition of transition strips at the leading edge is seen to have improved considerably both the consistency of the data and the agreement with the wind tunnel $-C_p$min values. Similar improvement was obtained for the other leading edge upper surface cases with the addition of transition strips. The situation is also generally similar for the leading edge, lower surface cavitation cases shown in Figures 17, 18 and 19.

For the mid-back cavitation case shown in Figure 16 for $0°\alpha$, $0°\delta$, there are again systematic data available for all three water tunnel test conditions. There is substantial agreement in the inception values between the three sets of water tunnel data although these are consistently lower than the corresponding $-C_p$min values from the wind tunnel. One significant difference which occurred with the addition of transition strips was a change in location of the cavitation from the flap hinge-line to the mid-back of the section. Figure 22 shows the appearance at cavitation inception for this condition at a Reynolds number of 2.5×10^6. Visual observation shows that the leading edge beads generated macroscopic bubbles which swept aft in the flow. As tunnel pressure was reduced to reach the critical cavitation number, these bubbles expanded suddenly to give the condition shown. There is no mid-back cavitation over the inner 2" of the span where there is no transition strip, although the cavitation has spread along the flap hinge-line in this region. Cavitation at the ends of the span is considered to have arisen from interference effects and has been consistently ignored.

The $+1°\alpha$, $0°\delta$ case is at a corner of the cavitation envelope, Figure 23, where the origin of the cavitation changes from mid-back to the leading edge. Consequently, the probability of premature cavitation at the leading edge due to the presence of the transition strip is comparatively large. Such cavitation did occur, as illustrated by the 'C' strip points at Re = 1.27 and 2.07×10^6, shown in Figure 15. The condition of the cavitation at inception is illustrated in Figure 24 for a Reynolds number of 2.5×10^6 and transition strip D. The bright leading edge is due mostly to light reflection from the glass beads but some cavitation is apparent. Critical cavitation number for inception over the mid-back was clearly defined under these circumstances but cavitation from the beads built slowly

and was influenced by irregularities and deterioration of the transition strips. Improvement in the technique of application, together with reduction to a minimum of the size and number of roughness particles, may substantially decrease the magnitude of discrepancies arising at the corners of the cavitation envelope.

The cavitation envelope of Figure 23 gives an overall picture of the magnitude and significance of the discrepancies found in the experimental data. The wind tunnel $-C_{p_{min}}$ values are plotted as a solid line and are assumed to give the best estimate of the cavitation envelope. The transition-fixed water tunnel data are in excellent agreement with this line. The transition-free water tunnel data, on the other hand, give a much more optimistic estimate of cavitation envelope width at low angles of attack. Since low angles of attack are typical of sub-cavitating hydrofoil operation at high speed, this discrepancy has important full scale implications.

5. CONCLUSIONS

Tests of flapped 16-309 section models in both water and wind tunnels have brought into sharp relief the relative advantages and limitations of these two different types of facility. The relatively large size of the wind tunnel model allows it to be constructed with better accuracy and surface smoothness ratio. Also, conditions are much easier for measurements and for flow analysis, so that the wind tunnel can provide more definitive force, moment and pressure data for the available Reynolds number range. It can also provide the good understanding of prevailing flow conditions often essential to successful data analysis.

The ability to observe cavitation characteristics and their effect on the forces generated is the great advantage of the water tunnel. However, the small size of the model makes high profile accuracy hard to achieve, and measurements are generally more difficult to make. Perhaps more important is the effect of the quality of the water flow. For water tunnel cavitation experiments, the nucleii content and flow turbulence are generally considered the most important factors. In the experiments discussed in this report, significant differences and inconsistencies occurred in the section characteristics as measured in the wind and water tunnels and between successive series of water tunnel tests on the same model. Differences in the free stream flow characteristics are thought to have played an important part in this.

The 16-309 section is very susceptible to flow separation near the trailing edge and this is dependent in turn on transition to turbulent flow. Despite the fact that it is a "laminar flow" type of section, turbulent flow conditions are much more likely to prevail under the practical sea conditions experienced by a hydrofoil. More nearly representative characteristics are therefore obtained in the wind tunnel with the application of roughness strips at the leading edge.

In the water tunnel case, turbulent flow over the model was achieved more readily than in the wind tunnel, at least in Series I tests. Nevertheless there were significant discrepancies between the water tunnel cavitation inception characteristics and theoretical characteristics, as indicated by wind tunnel pressure measurements. These discrepancies became even greater for Series II tests, for which tunnel free-stream turbulence was apparently reduced as a result of modifications and improvements to the tunnel hydraulic circuit. Again, application of roughness strips at the model leading edge resulted in the achievement of cavitation inception values much closer to those indicated by wind tunnel tests. An exception was for angle settings close to the corners of the cavitation envelope, where the pressure envelope is comparatively flat and small changes to the leading edge profile can prove significant. Even here, however, refinements in the character and application of the transition strips could probably improve the results.

TABLE 1: WIND-TUNNEL EXPERIMENTS (FROM REFERENCE 1)

FLAP ANGLE, δ						Re	FLAP HINGE SEALED	TRANSITION STRIPS ON	PRESSURE DATA TAKEN
-10°	-4°	0°	+6°	+10°	+15°	$x10^{-6}$			
x	x	x	x	x	x	1.90			
		x				.86			
x	x	x	x	x	x	4.05			
			x			4.87			
x	x	x	x	x	x	1.90	x		x
x	x	x	x	x	x	4.05	x		x
		x				1.90	x	x	x
		x	x			4.05	x	x	x

Angle of attack, α: At least every 1 degree between α = -4 deg. and α = 6 deg.

TABLE 2: WATER TUNNEL EXPERIMENTS, SERIES 1
(FROM REFERENCE 2)

FLAP ANGLE, δ, DEG.	NOMINAL Re x10^{-6}					ANGLE OF ATTACK, α, DEG.											CAVITATION (C) OR Re (R) SURVEY
	1.25	2.0	2.5	3.5	4.0	-5	-4	-3	-2	-1	0	1	2	3	4	6	
-10			x								x	x					C
-5			x						x		x	x					C
0			x				x		x	x	x	x	x		x	x	C
2.5			x			x	x		x		x	x	x			x	C
5			x				x	x	x	x	x	x	x	x			C
7.5			x			x	x		x		x	x	x				C
10			x			x	x		x	x	x	x	x	x			C
0	x	x	x	x	x						x		x				R
5	x	x	x	x	x						x		x				R

TABLE 3: WATER TUNNEL EXPERIMENTS, SERIES 2

ANGLE OF ATTACK, δ, DEG.	FLAP ANGLE, α, DEG.		NOMINAL Re x 10^{-6}											
	0	5	1.25	1.30	2.00	2.15	2.50	2.65	3.00	3.20	3.50	3.75	4.00	4.20
-4	x		x	x	x	x	x	x	x					
-3	x			x		x		x						
-2	x		x	x	x	x	x	x	x	x	x		x	
-1	x			x		x		x		x				
0	x		x	x	x	x	x	x	x	x	x		x	
1	x		x	x	x	x	x	x	x	x	x	x	x	x
2	x		x	x	x	x	x	x	x	x	x		x	
3	x		x	x	x	x	x	x	x	x	x			
4	x		x	x	x	x	x	x	x	x				
-4		x	x		x		x		x					
-3		x	x		x		x		x		x			
-2		x	x		x		x		x		x			
-1		x	x		x		x		x		x			
0		x	x	x	x		x		x		x			
1		x	x	x	x	x	x	x	x	x	x	x		
2		x	x	x	x	x	x	x	x					
3		x	x		x		x							
4		x	x		x		x							

The spread of Reynolds number in a few of these tests was high, some being made at intermediate values: they have been reported in this table at the nearest nominal value.

TABLE 4: SYMBOL CHART FOR CAVITATION INCEPTION DIAGRAMS

SERIES I	SERIES II		CAVITATION LOCATION
	TRANS. FIXED	TRANS FREE	
◇	◆	◇	LDG EDGE UPPER
△	▲	△	LDG EDGE LOWER
□	■	□	MID-BACK UPPER
○	●	○	HINGE-LINE UPPER

◯ RINGED DATA ARE FOR $-C_p$min WITH FIXED TRANSITION

Fig. 1: View of Wind Tunnel Model

Model with fairing plate installed, ready for installation in working section.

Fig. 2: Water Tunnel Model

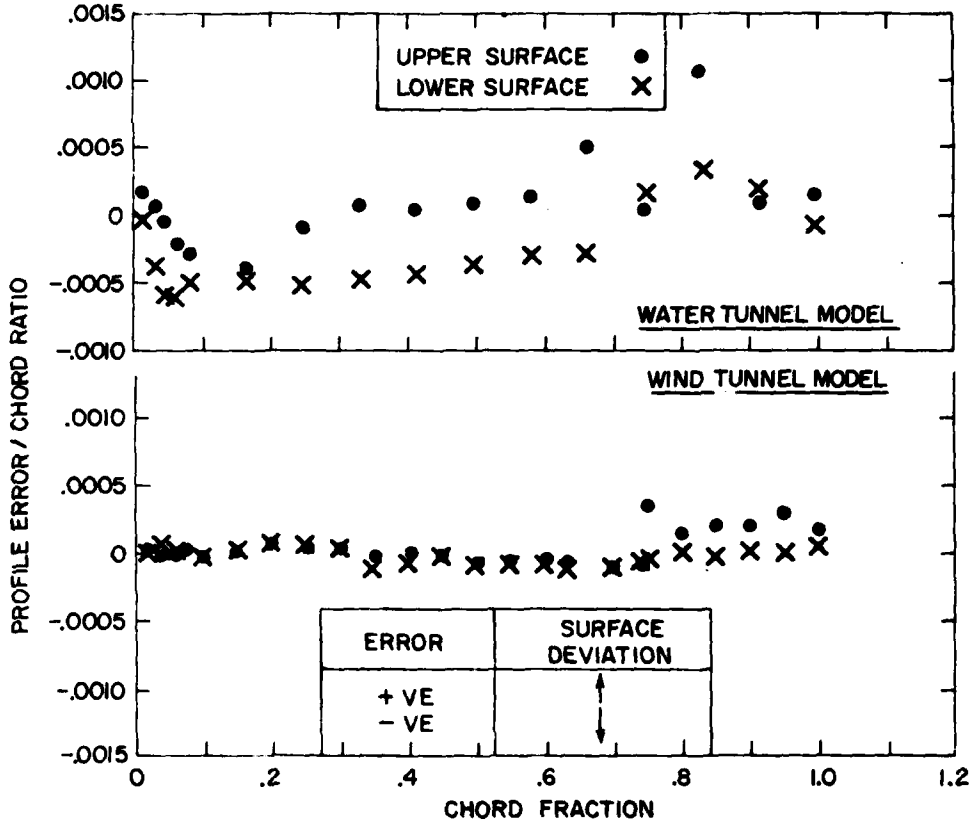

FIG. 3: PROFILE ERROR MEASUREMENTS

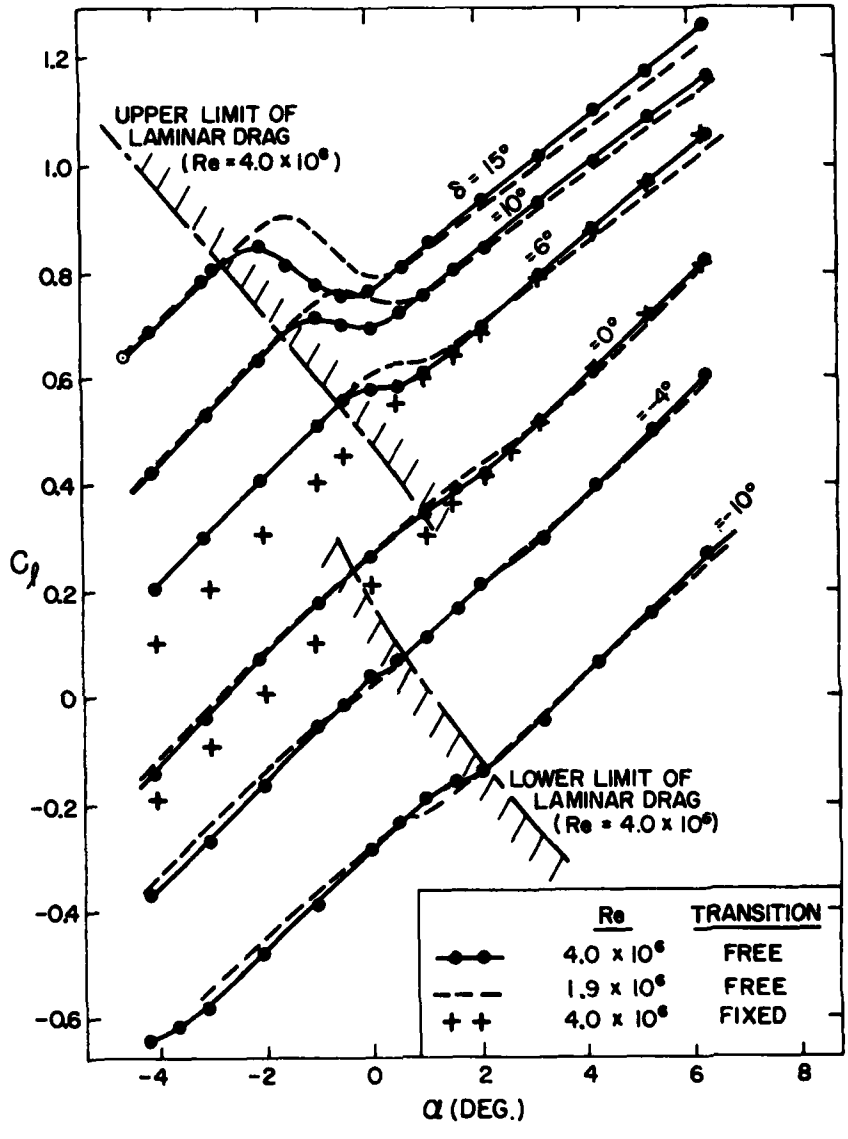

FIG. 3: WIND TUNNEL SECTION LIFT CHARACTERISTICS

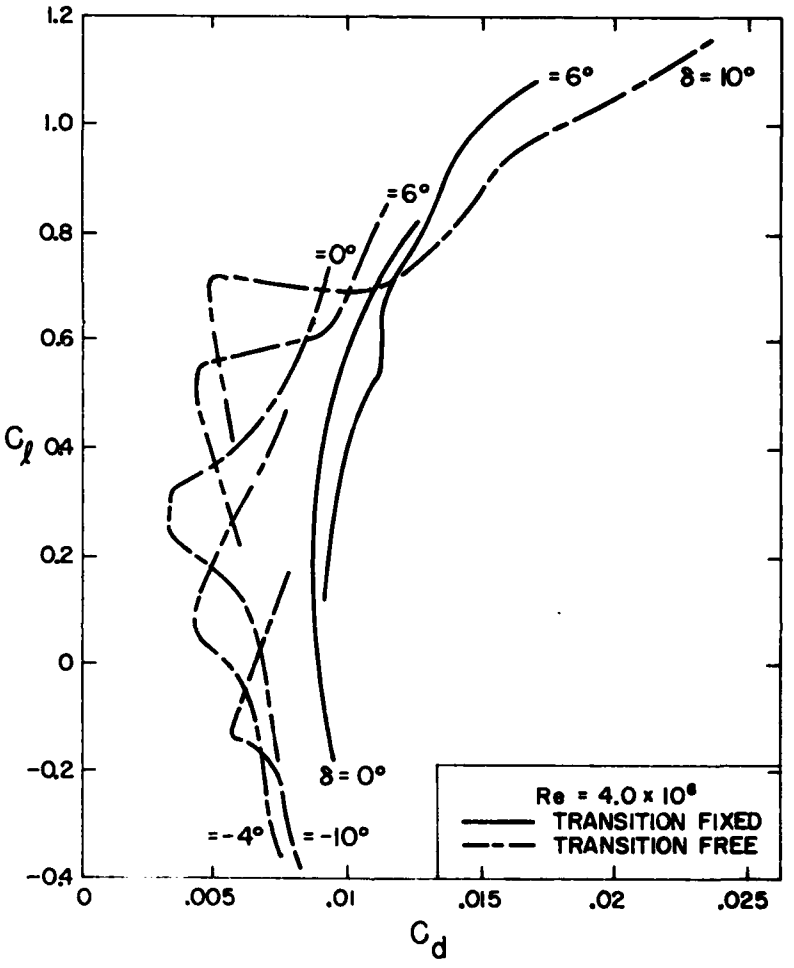

FIG. 5: WIND TUNNEL DRAG CHARACTERISTICS

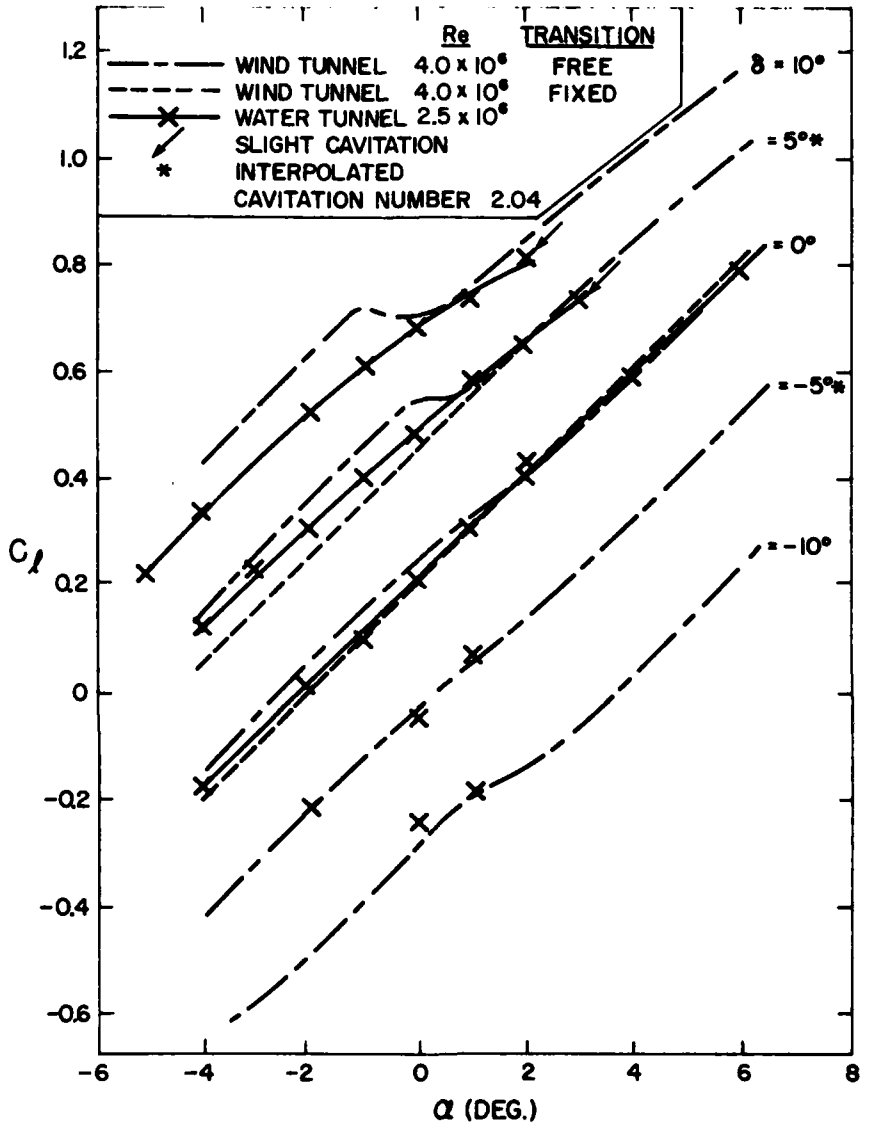

FIG. 6: COMPARISON OF LIFT CHARACTERISTICS

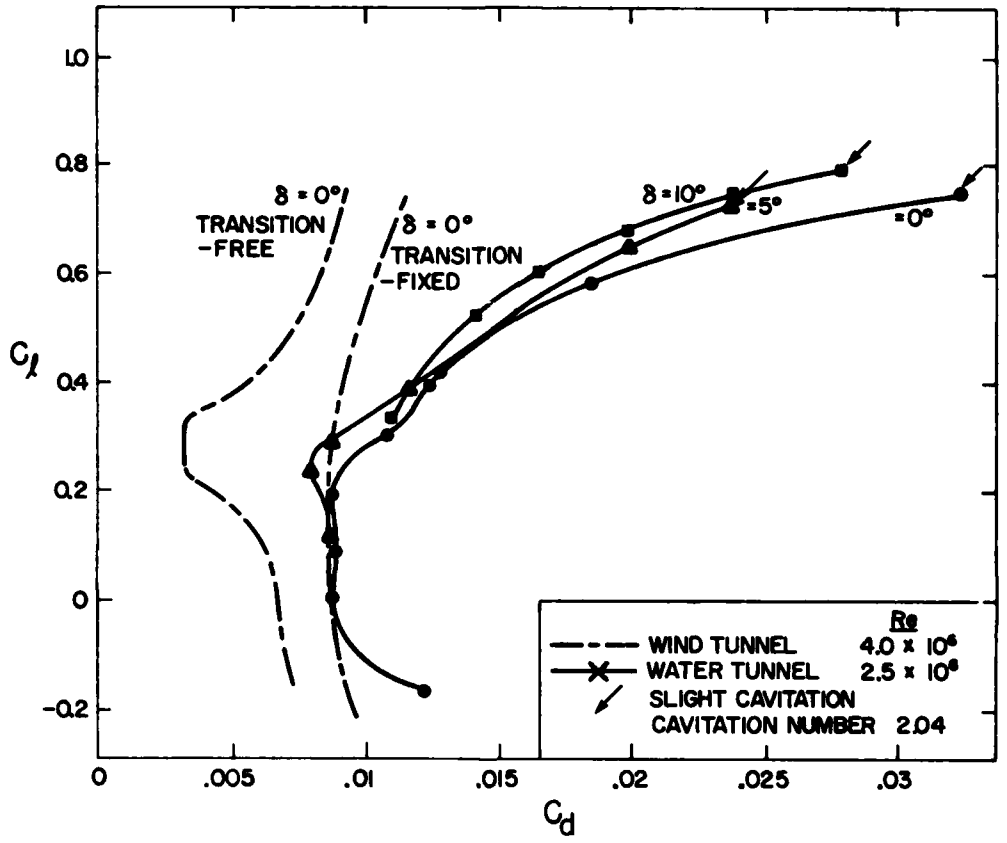

FIG. 7: COMPARISON OF DRAG CHARACTERISTICS

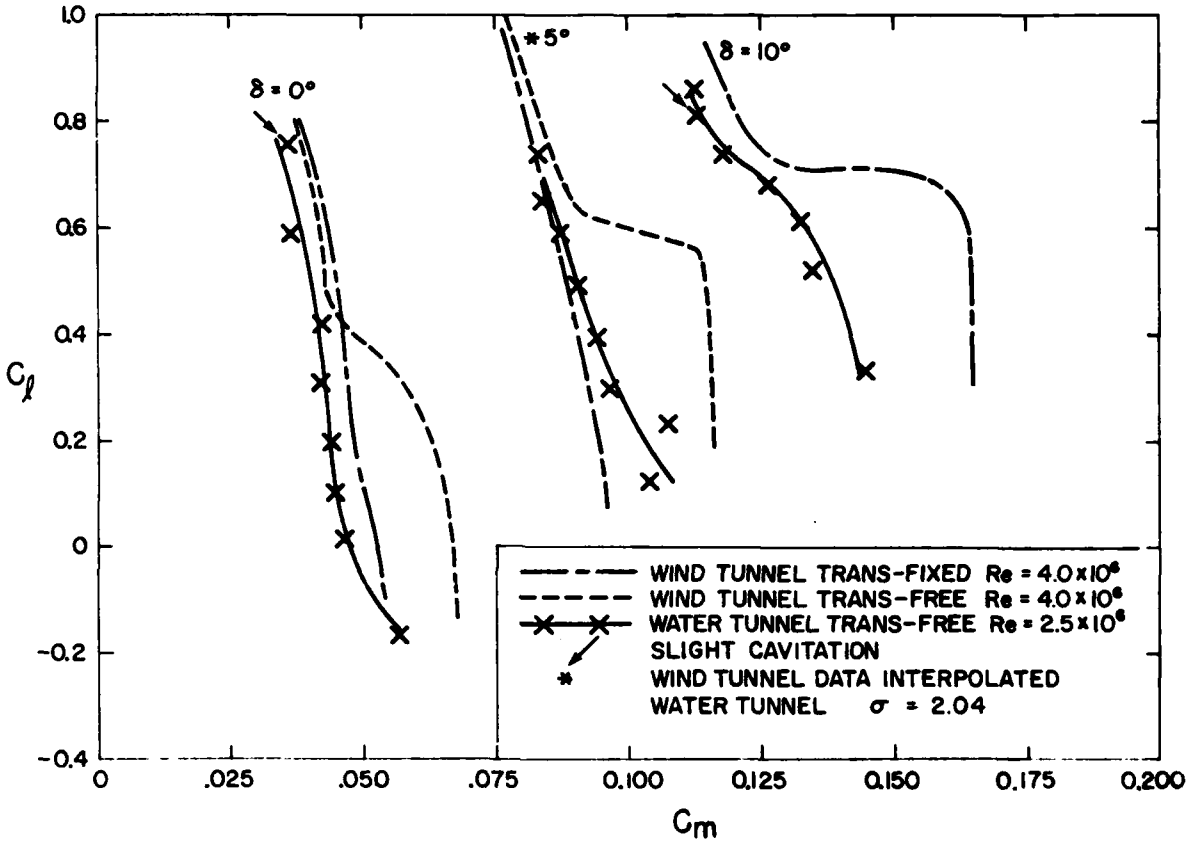

FIG. 8: COMPARISON OF MOMENT CHARACTERISTICS

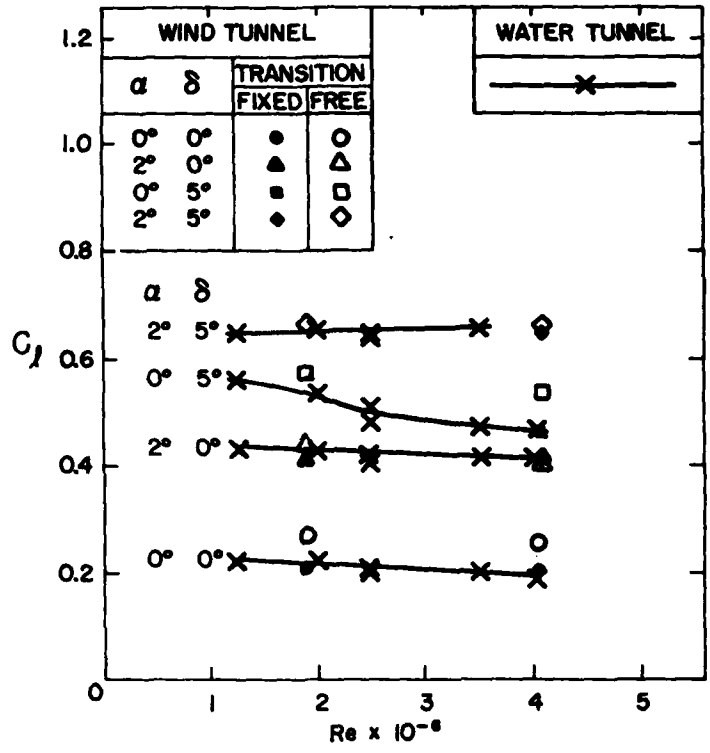

FIG. 9: UNCAVITATED LIFT COEFFT.-VS-REYNOLDS NO.

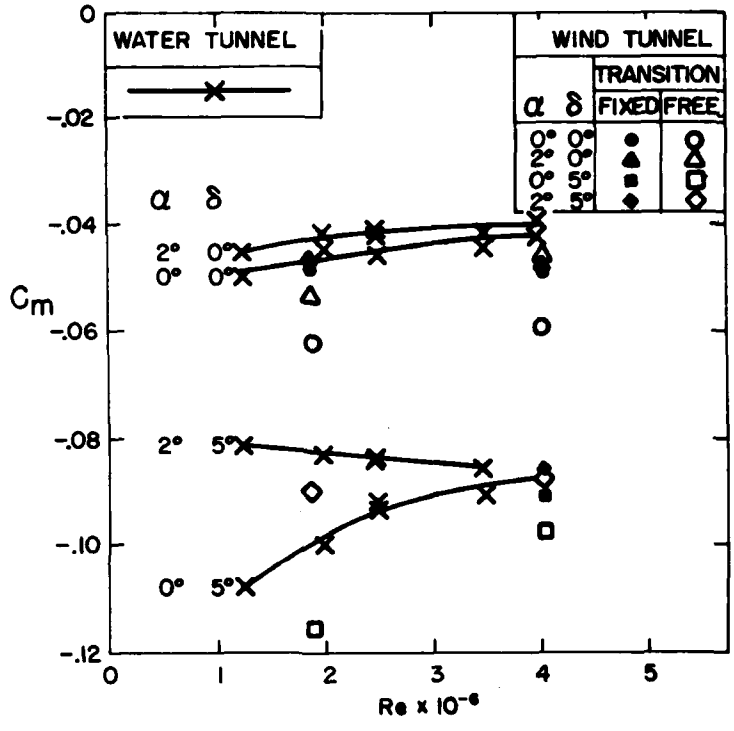

FIG. 10: UNCAVITATED PITCHING MOMENT COEFFT.-VS-REYNOLDS NO.

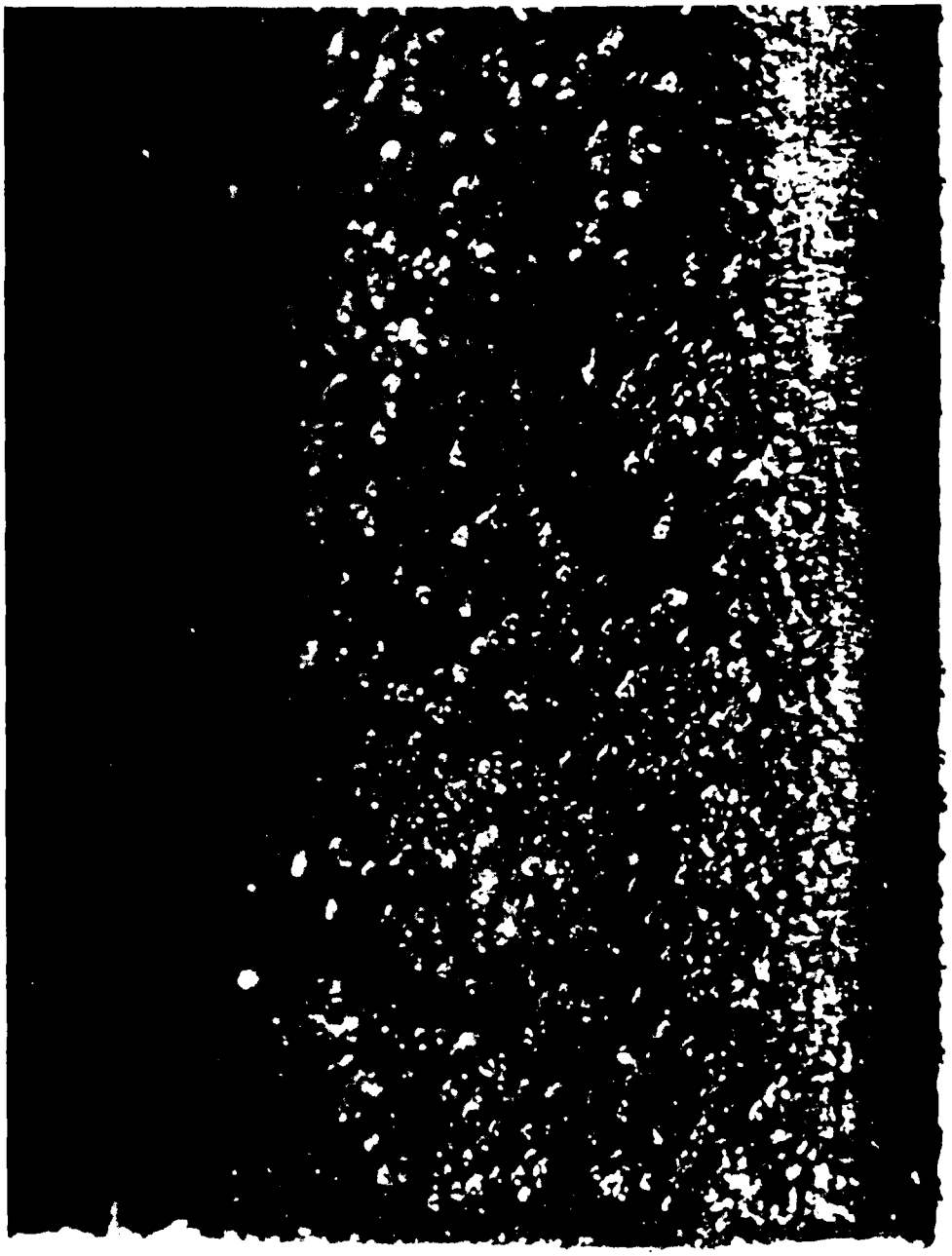

Fig. 11: Roughness Strip: A Typical Bead Dispersion

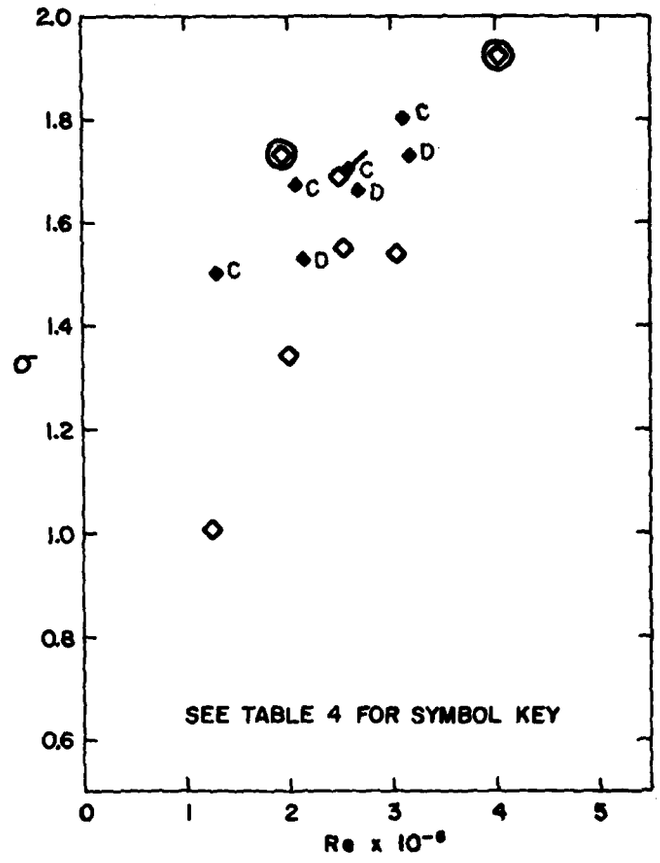

FIG. 12: CAVITATION INCEPTION AT 4°α 0°δ

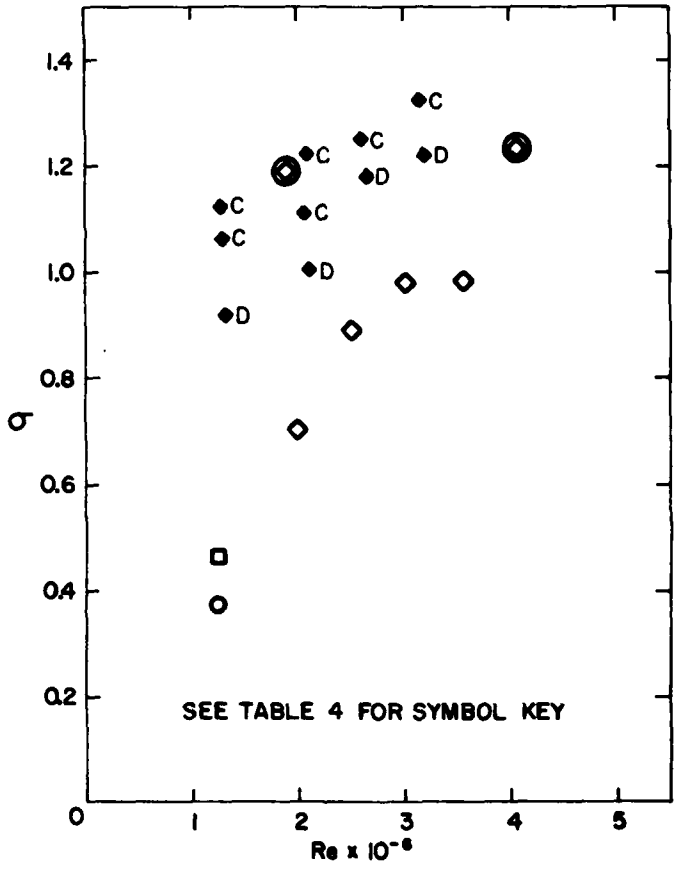

FIG. 13: CAVITATION INCEPTION AT 3°α 0°δ

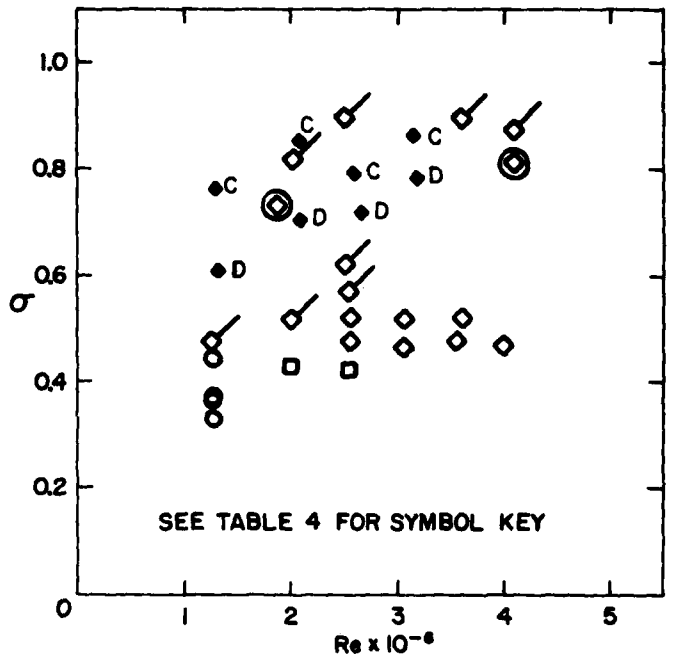

FIG. 14: CAVITATION INCEPTION AT 2°α 0°δ

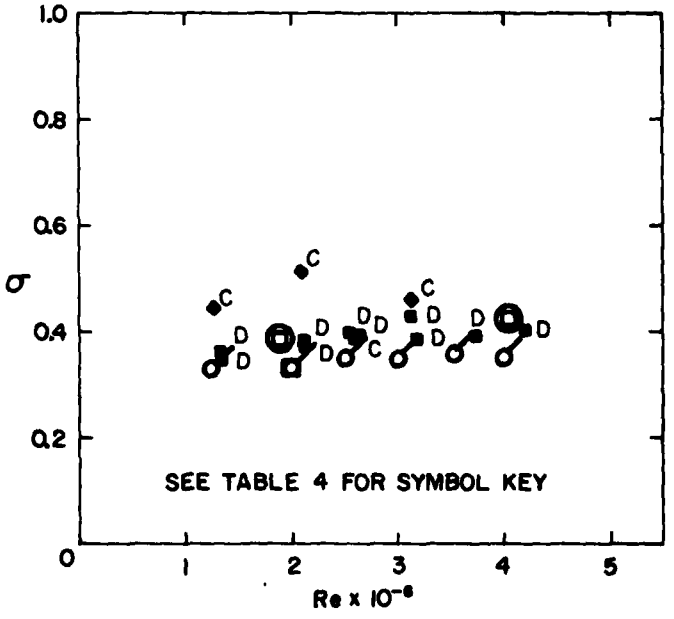

FIG. 15: CAVITATION INCEPTION AT +1°α 0°δ

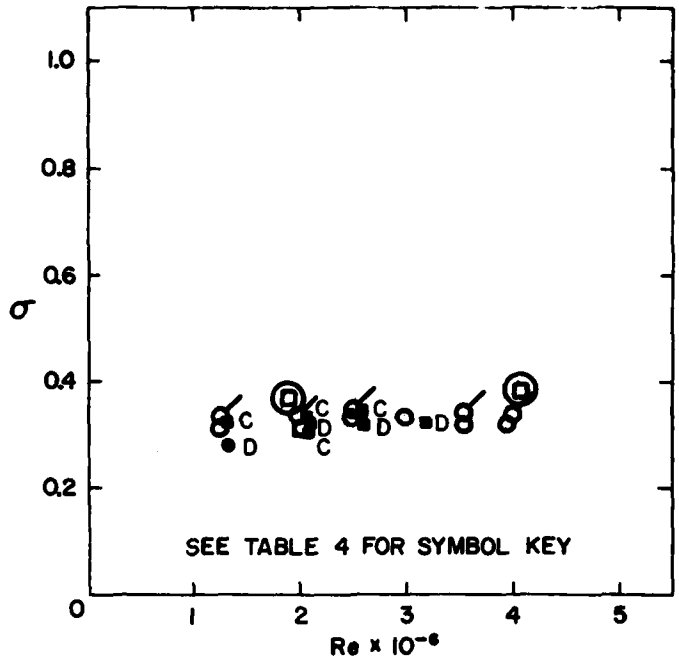

FIG. 16: CAVITATION INCEPTION AT 0°α 0°δ

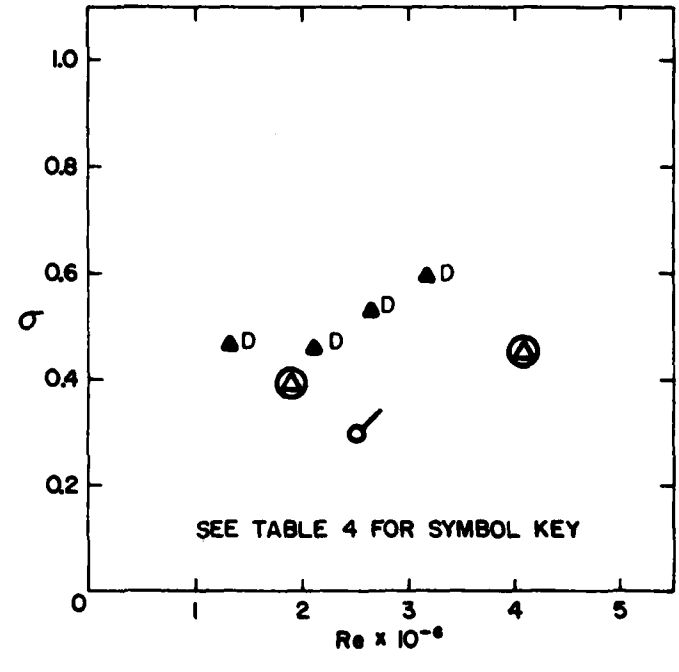

FIG. 17: CAVITATION INCEPTION AT -1°α 0°δ

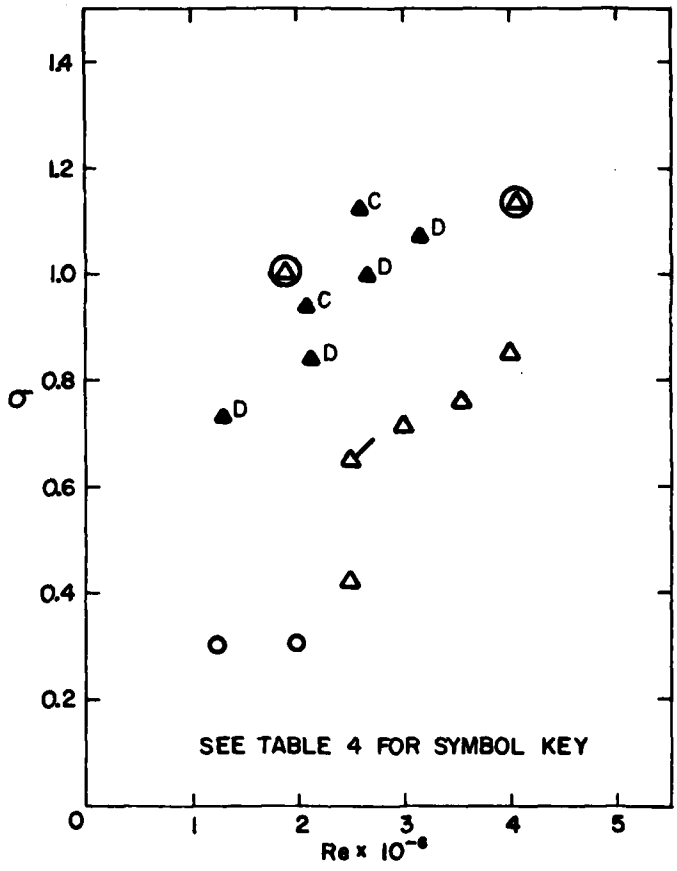

FIG. 18: CAVITATION INCEPTION AT -2°α 0°δ

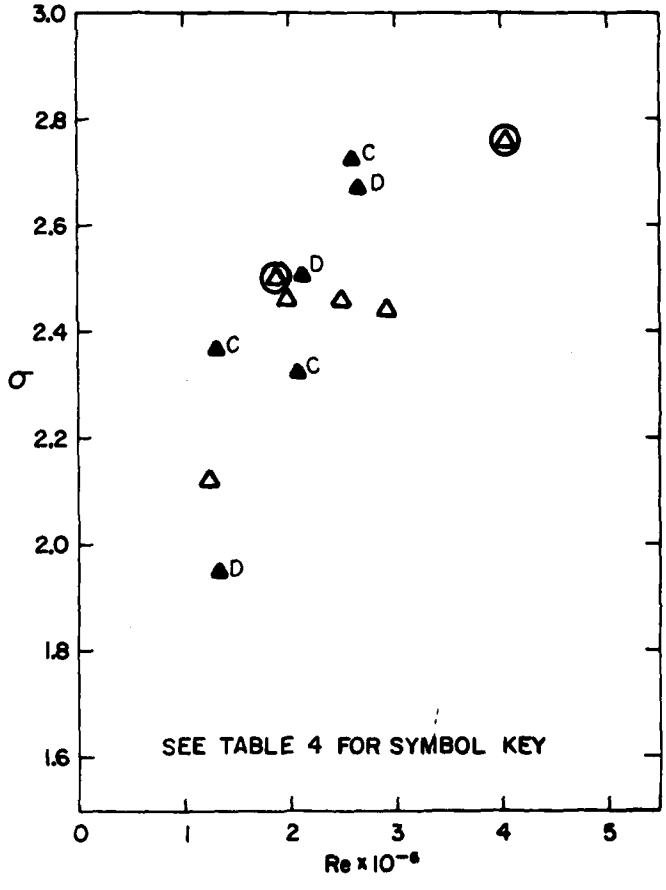

FIG. 19: CAVITATION INCEPTION AT -4°α 0°δ

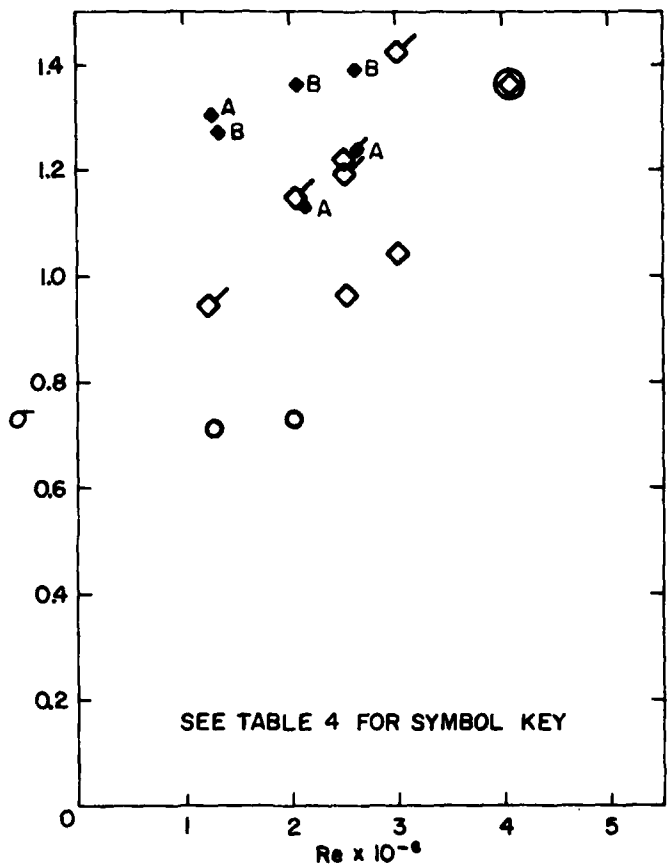

FIG. 20: CAVITATION INCEPTION AT 2°α 5°δ

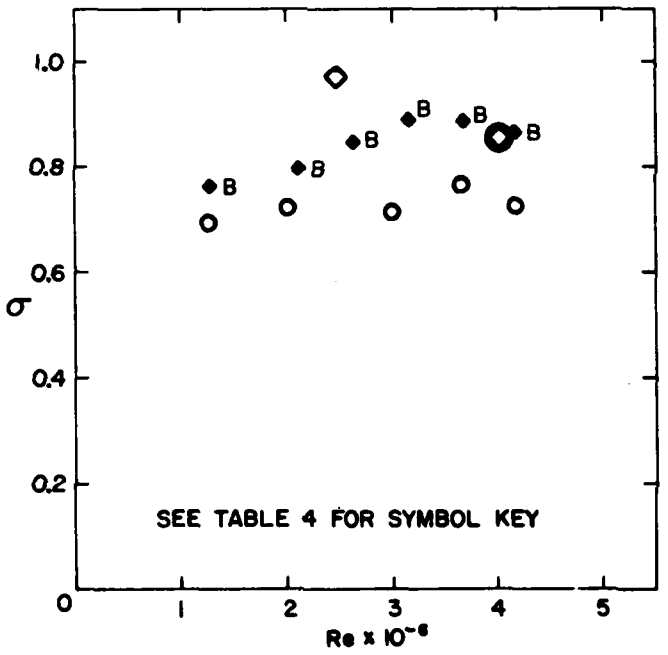

FIG. 21: CAVITATION INCEPTION AT 1°α 5°δ

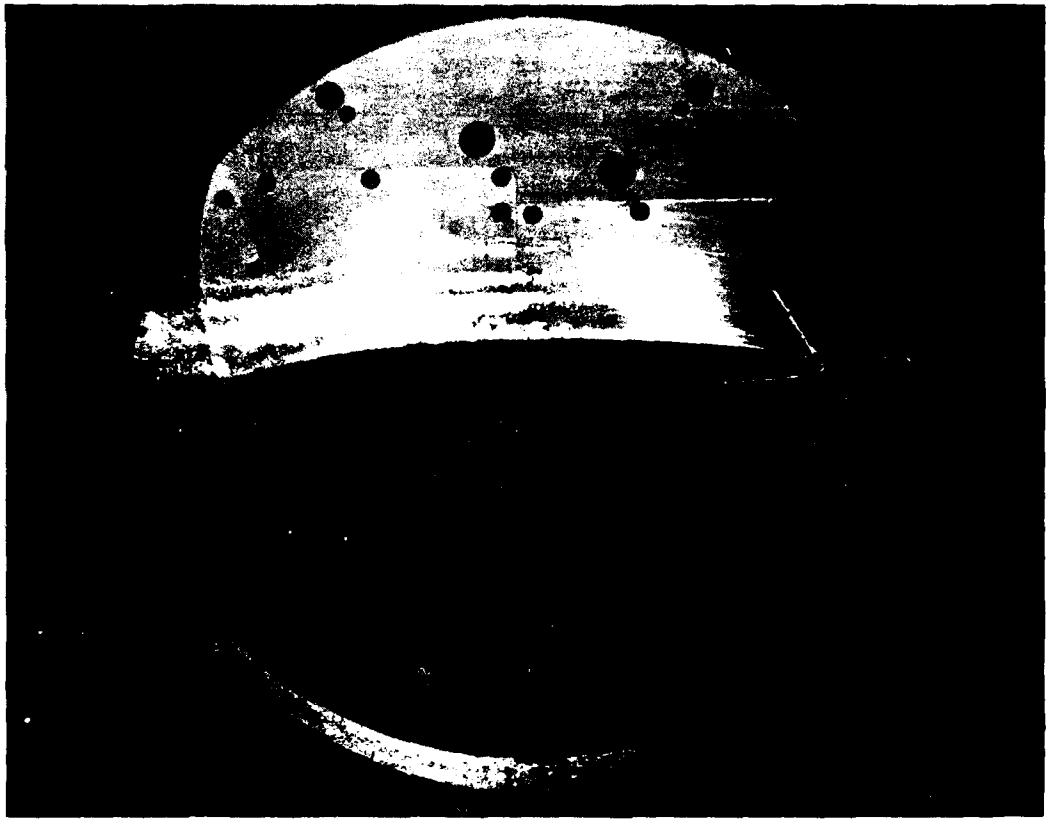

Fig. 22: $0°\alpha$ $0°\delta$ Re = 2.5×10^6
Condition at Mid-Back Cavitation Inception

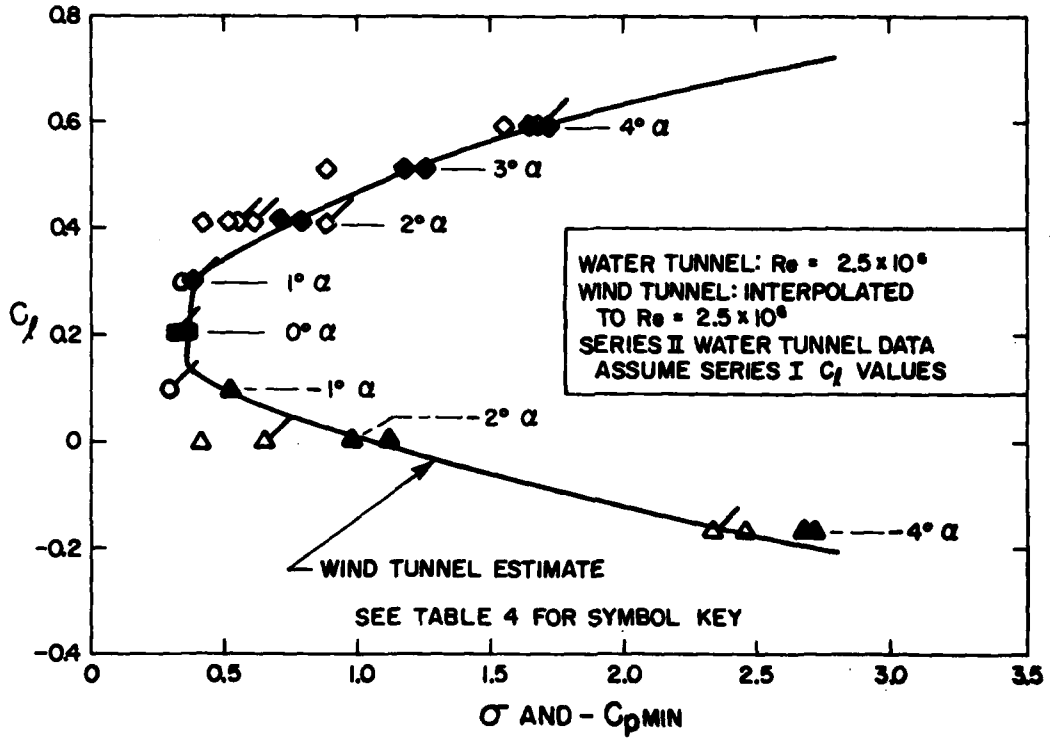

FIG. 23: CAVITATION ENVELOPE FOR 0° FLAP ANGLE

Fig. 24: $1°\alpha\ 0°\delta$ $Re = 2.5 \times 10^6$
Condition at Mid-Back Cavitation Inception

REFERENCES

1. Teeling, P.: "Low Speed Wind Tunnel Tests on a NACA 16-309 Section with Trailing Edge Flap", DeHavilland Aircraft of Canada, Ltd. Report 76-3, October 1976, for Defence Research Establishment Atlantic, P.O. Box 1012, Dartmouth, N.S., Canada.

2. Jones, E.A. and Mackay, M.: "Water Tunnel Tests on a NACA 16-309 Section Equipped with a Simple, Sealed Flap". Technical Memorandum 79/C, Defence Research Establishment Atlantic, P.O. Box 1012, Dartmouth, N.S., Canada.

3. Ward, T.M.: "The Hydrodynamics Laboratory at the California Institute of Technology - 1976", Graduate Aeronautical Laboratories, CIT, Pasadena, California, January 1976.

4. Wardlaw, R.L.: "The National Aeronautical Establishment's 6 ft x 9 ft Low Speed Wind Tunnel", Canadian Aeronautics and Space Journal, Vol. 9, No. 4, April 1963.

UNCLASSIFIED

Security Classification

DOCUMENT CONTROL DATA - R & D

(Security classification of title, body of abstract and indexing annotation must be entered when the overall document is classified)

1. ORIGINATING ACTIVITY Defence Research Establishment Atlantic	2a. DOCUMENT SECURITY CLASSIFICATION UNCLASSIFIED 2b. GROUP

3. DOCUMENT TITLE

"MODEL SCALE EFFECTS ON A 16-309 FLAPPED HYDROFOIL SECTION"

4. DESCRIPTIVE NOTES (Type of report and inclusive dates)
Technical Memorandum

5. AUTHOR(S) (Last name, first name, middle initial)

ERIC A. JONES

6. DOCUMENT DATE April 1980	7a. TOTAL NO. OF PAGES 44	7b. NO. OF REFS 4
8a. PROJECT OR GRANT NO.	9a. ORIGINATOR'S DOCUMENT NUMBER(S) DREA Technical Memorandum 80/B	
8b. CONTRACT NO.	9b. OTHER DOCUMENT NO.(S) (Any other numbers that may be assigned this document)	

10. DISTRIBUTION STATEMENT

As per attached list.

11. SUPPLEMENTARY NOTES	12. SPONSORING ACTIVITY DREA

13. ABSTRACT

Wind and water tunnel tests have been conducted of a NACA 16-309 section with the standard a = 1.0 camber line and equipped with a 25% flap-chord ratio, simple, sealed flap. Differences between test results from the two facilities are discussed, as well as the effect of placing roughness strips near the leading edge. Results are given showing the dependency of force, moment and, in particular, cavitation inception on Reynolds number over the range from 1.25×10^6 to 4.0×10^6.

DSIS
78-079

KEY WORDS

wind tunnel tests
water tunnel tests
NACA 16-309 section
flap
cavitation
Reynolds number

INSTRUCTIONS

1. ORIGINATING ACTIVITY: Enter the name and address of the organization issuing the document.

2a. DOCUMENT SECURITY CLASSIFICATION: Enter the overall security classification of the document including special warning terms whenever applicable.

2b. GROUP: Enter security reclassification group number. The three groups are defined in Appendix 'M' of the DRB Security Regulations.

3. DOCUMENT TITLE: Enter the complete document title in all capital letters. Titles in all cases should be unclassified. If a sufficiently descriptive title cannot be selected without classification, show title classification with the usual one-capital-letter abbreviation in parentheses immediately following the title.

4. DESCRIPTIVE NOTES: Enter the category of document, e.g. technical report, technical note or technical letter. If appropriate, enter the type of document, e.g. interim, progress, summary, annual or final. Give the inclusive dates when a specific reporting period is covered.

5. AUTHOR(S): Enter the name(s) of author(s) as shown on or in the document. Enter last name, first name, middle initial. If military, show rank. The name of the principal author is an absolute minimum requirement.

6. DOCUMENT DATE: Enter the date (month, year) of Establishment approval for publication of the document.

7a. TOTAL NUMBER OF PAGES: The total page count should follow normal pagination procedures, i.e., enter the number of pages containing information.

7b. NUMBER OF REFERENCES: Enter the total number of references cited in the document.

8a. PROJECT OR GRANT NUMBER: If appropriate, enter the applicable research and development project or grant number under which the document was written.

8b. CONTRACT NUMBER: If appropriate, enter the applicable number under which the document was written.

9a. ORIGINATOR'S DOCUMENT NUMBER(S): Enter the official document number by which the document will be identified and controlled by the originating activity. This number must be unique to this document.

9b. OTHER DOCUMENT NUMBER(S): If the document has been assigned any other document numbers (either by the originator or by the sponsor), also enter this number(s).

10. DISTRIBUTION STATEMENT: Enter any limitations on further dissemination of the document, other than those imposed by security classification, using standard statements such as:

(1) "Qualified requesters may obtain copies of this document from their defence documentation center."

(2) "Announcement and dissemination of this document is not authorized without prior approval from originating activity."

11. SUPPLEMENTARY NOTES: Use for additional explanatory notes.

12. SPONSORING ACTIVITY: Enter the name of the departmental project office or laboratory sponsoring the research and development. Include address.

13. ABSTRACT: Enter an abstract giving a brief and factual summary of the document, even though it may also appear elsewhere in the body of the document itself. It is highly desirable that the abstract of classified documents be unclassified. Each paragraph of the abstract shall end with an indication of the security classification of the information in the paragraph (unless the document itself is unclassified) represented as (TS), (S), (C), (R), or (U).

The length of the abstract should be limited to 20 single-spaced standard typewritten lines; 7½ inches long.

14. KEY WORDS: Key words are technically meaningful terms or short phrases that characterize a document and could be helpful in cataloging the document. Key words should be selected so that no security classification is required. Identifiers, such as equipment model designation, trade name, military project code name, geographic location, may be used as key words but will be followed by an indication of technical context.